Polímeros
ISSN 1678-5169 (Online)

https://doi.org/10.1590/0104-1428.20220075

ORIGINAL ARTICLE

Conductive Amazon açaí/polyaniline composite fiber: fabrication and properties

Jefter Victor Gonçalves[1], Jefferson Suela[1], Marcus Vinícius Duarte Silva[1], Rodrigo Fernando Bianchi[2] and Cleidinéia Cavalcante da Costa[1,2]*

[1]Departamento de Física, Instituto Federal de Minas Gerais, Congonhas, MG, Brasil
[2]Laboratório de Polímeros e de Propriedades Eletrônicas de Materiais, Departamento de Física, Universidade Federal de Ouro Preto, Ouro Preto, MG, Brasil
cleidineiastm@gmail.com

Abstract

This paper investigates the properties of the polyaniline (PANI) on açaí vegetable fiber (AVF), hereafter referred to as PANI-COATED:AVF. Scanning electron and atomic force microscopy showed that the incorporation of PANI produced a linear surface, while optical microscopy images showed that the semiconductor layer was flawed. The complex impedance measurements performed at room temperature indicated that the electrical properties of PANI were fully transferred to the PANI-COATED:AVF and that the Cole-Cole approach dominated over a frequency range from 1 Hz to 100 kHz. Thermogravimetric analysis revealed a thermal stability range of 0° to 300°C. Finally, the combination of PANI with AVF was a successful due to the ease of processing and obtaining semiconductor filaments with wide ranges of thermal and electrical stability. This article is a complement to another recently published [doi.org/10.1002/pc.27068].

Keywords: *natural polymer, semiconducting polymer, environmental conservation.*

How to cite: Gonçalves, J. V., Suela, J., Silva, M. V. D., Bianchi, R. F., & Costa, C. C. (2023). Conductive Amazon açaí/polyaniline composite fiber: fabrication and properties. *Polímeros: Ciência e Tecnologia*, *33*(4), e20230037. https://doi.org/10.1590/0104-1428.20220075

1. Introduction

The largest natural reserves of açaí palm (*Euterpe oleracea* Mart.) can be found in the state of Para, Brazil[1-4]. The harvesting of the fruit of this species native to Amazonia contributes to the livelihood of local families[2]. The fruit of the açaí palm, which is generally discarded incorrectly in nature[5], consists of seeds covered by lignocellulosic vegetable fibers (AVF)[6]. These AVF are renewable resources, biodegradable, low-cost[7], and have multi-functional and environmentally friendly applications[8]. For example, AVF can be used as pH sensors in the food industry[9], and mechanical reinforcement elements of polymeric matrices[5,10,11]. Furthermore, AVF can be added to the polyaniline (PANI) in situ chemical synthesis route to expand on its potential biotechnological applications[8,12-14] and obtain AVF coated with protonated PANI[15,16] (PANI-COATED:AVF) to be used as structural elements of electronic devices[13,17,18].

The goal of this paper is to describe in detail the method for producing PANI-COATED:AVF and analyze the morphological, thermal, and electrical properties provided by the semiconductor coating. This would provide a novel alternative source of income for the needy population by promoting environmental sustainability.

2. Materials and Methods

2.1 Preparation of PANI-COATED:AVF

Figure 1 shows images of the preparation of açaí vegetable fibers (AVF) before acquiring the PANI layer. The AVF were obtained in the Açaizal community, 32 kilometers from the Santarém-Curuá-Una highway, in Brazil, from an Amazonian palm (Euterpe *oleraceae* Mart.)[19] (Figure 1a). Its fruit is the açaí (Figure 1b) which becomes a waste product after pulping (Figure 1c). In this situation, the AVF were separated from the seeds (Figure 1d), sifted in a 32 mesh sieve (Figure 1e), and those with diameters of 0.3 ± 0.2 mm and length of 3.0 ± 1.0 mm were selected (Figure 1f).

In this study, the PANI was synthesized through the direct oxidation of aniline by chemical oxidants, based on the PANI synthesis procedure[15,16]. The process for the fabrication of the PANI under AVF, hereafter referred to as PANI-COATED:AVF. Following the PANI synthesis, 0.6 g of AVF were mixed with 300 mL of hydrochloric acid (HCl) 1 M and left at room temperature (24 ºC). The next day, 20 mL of distilled aniline was diluted in the mixture. In a second beaker, 11.52 g ammonium persulfate ($(NH_4)_2S_2O_8$) was added to 200 mL HCl (1 M). Both solutions were placed

Figure 1. Preparation of acai vegetable fibers (AVF). (a) Amazonian palm; (b) açaí fruit; (c) açaí waste after depulping; (d) AVF; (e) AVF sieving; (f) AVF with a length of 3.0 ± 1.0 mm.

into a freezer and removed when at a temperature of around 0°C. The solutions were slowly combined in a 1000 mL beaker, insulated with aluminum, and mixed together through stirring for 2 hours at 24 °C. The PANI solution in the form of protonated emerald salts was washed with acetone several times and finally cleaned with a filter paper, and a polymeric bulk was obtained. After about 48 hours in a desiccator, the PANI-COATED:AVF was separated from the PANI powder by sieving.

2.2 Experimental characterization

The surface morphologies of the AVF and PANI-COATED:AVF were studied by scanning electron microscopy (SEM), atomic force microscopy (AFM), and optical microscopy (OM). The SEM images were obtained with a Tescan Vega LM3 microscope. The AFM images were acquired using a Ntegra Prima (NT-MDT) microscope operating in intermittent contact mode with regular Si cantilevers (k ~10 N/m, f0 ~240 kHz). The OM images were taken with a ZEISS Stemi 2000-C microscope.

The polymers AVF, PANI, and PANI-COATED:AVF were thermally decomposed by thermogravimetric analysis (TGA). The thermal behavior was monitored on a TG instrument SDT 2960 at 10°C/min from room temperature to 700°C under a N_2 flow.

For electrical characterization, the polymers (AVF, PANI, and PANI-COATED:AVF) were pressed to obtain pellets with thicknesses of 1.0 ± 0.2 mm using a stainless steel apparatus coupled to a hydraulic model SKAY. Then, the pellets were kept between copper discs with circular openings (43.02 ± 2.32 mm^2) and gold-sputtered in a sputter coater (Balzers SCD 050) for 200 seconds. The complex impedance measurements, $Z^*(f) = Z'(f) - iZ''(f)$, were carried out using a 1260 Solartron frequency response analyzer in the 1 Hz to 10^5 Hz frequency range, maintaining the voltage amplitude at 1.5 V while experiments took place at room temperature.

3. Results and Discussions

Figure 2 shows the SEM images of AVF and PANI-COATED:AVF. The micrographs confirm that the surfaces of the AVF (Figure 2a) were rougher than those of the PANI-COATED:AVF (Figure 2b) which were smoother. The PANI layer covered the rough surface and parenchymal cells of the AVF[20].

The AFM images (Figure 3) complement the results presented in Figure 2 by providing greater detail with three-dimensional profiles which show the surface topography of the AVF (Figure 3a) as being more irregular than the surface of the PANI-COATED:AVF (Figure 3b). Furthermore, the surface topographic analysis provided a medium roughness value of 157 nm for the AVF (Figure 3a) and 71 nm for the PANI-COATED:AVF (Figure 3b). Therefore, the PANI layer significantly removed roughness in the surface of the AVF as observed by SEM (Figure 2) and AFM (Figure 3). The smoother fiber surface would lead to an improved resistance to contact with electrodes[21].

Figure 4 shows optical microscopy images of the surfaces of AVF and of PANI-COATED:AVF. The images of AVF show a homogeneous and continuous surface (Figure 4a) while the PANI-COATED:AVF exhibits a heterogeneous surface with failures in polymeric coating (Figure 4b). In contrast, Souza et al.[14] obtained a continuous coverage of

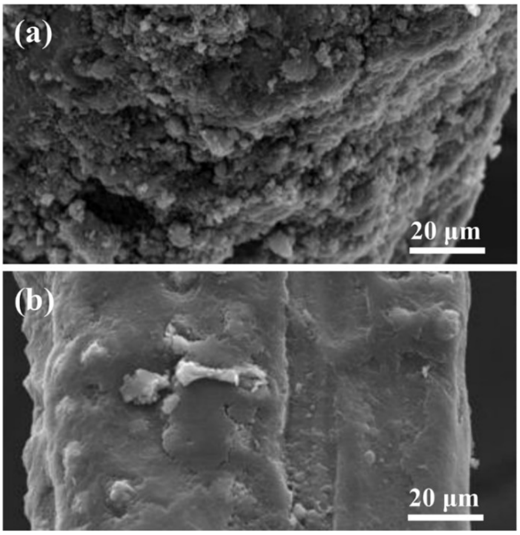

Figure 2. Scanning electron microscopy (SEM) images of (a) AVF and (b) PANI-COATED:AVF.

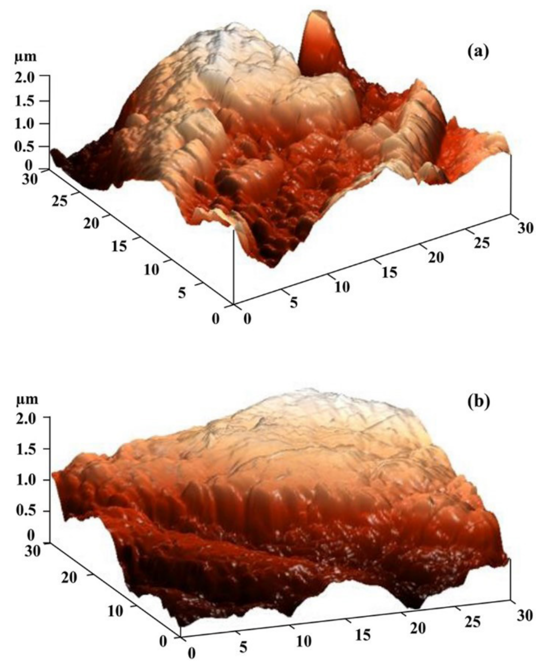

Figure 3. Atomic force microscopy (AFM) images of (a) AVF and (b) PANI-COATED:AVF.

PANI on VF, likely because the acidic solution in which the fibers were contained was magnetically stirred for 24 hours before the synthesis of PANI, allowing better incorporation of the acidic solution into the fibers. In this work, however, the fibers remained in the catalyst solution for 24 hours at a temperature of ≈0ºC. Indeed, the fibers filled with a catalyst solution would allow a more efficient polymerization of the surface, and the protonation could be characterized by the addition of Cl^- to N^+ or to other atoms[22].

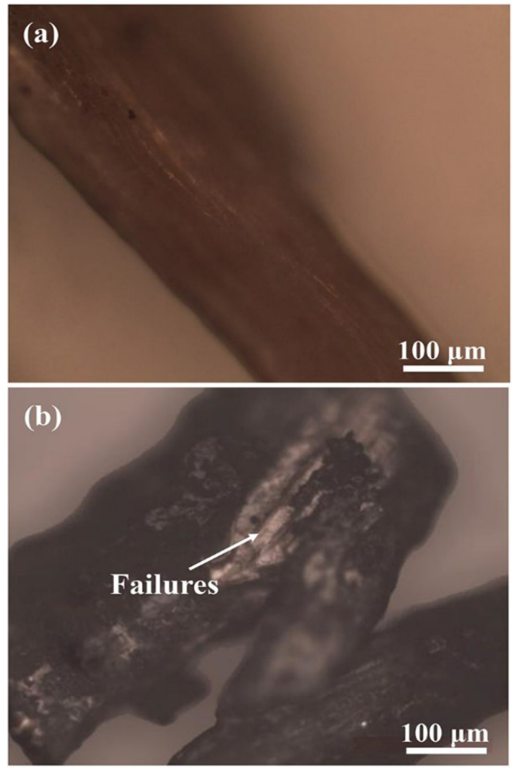

Figure 4. Optical microscopy (OM) images of (a) AVF and (b) PANI-COATED:AVF.

Figure 5 shows the TGA curves of the AVF, PANI, and PANI-COATED:AVF samples from room temperature to 700°C. Regarding the thermal degradation of AVF from 0ºC to 100ºC, about 10% of the mass was lost which could be attributed to water loss[5,14], the material then became thermally stable between 100ºC to 300ºC. From 300ºC to 400ºC, the mass loss was about 60% due to the thermal degradation characteristics of the AVF[20], caused by the decomposition of hemicellulose and β−(1−4) glycosidic linkages[23]. Finally, above 400ºC, the mass loss was about 10% due to the decomposition of lignin[5]. The thermogravimetric behavior of pure PANI showed a two-step mass loss. The first mass loss of around 10% from 0ºC to 100ºC represented water loss and the second mass loss of around 40% between 100ºC to 700°C was due to the degradation of dopant anions, removal of dopants, and decomposition of the PANI[24]. The TGA results of the PANI-COATED:AVF revealed that around 10% of water was released up to 100ºC. The combination of the PANI with the AVF provided an intermediate level of degradation to PANI-COATED:AVF due to the PANI surface layers[14]. A similar behavior of the thermogravimetry curves shown in Figure 5 has previously been observed[12].

Figure 6 displays the real, Z'(f), and imaginary, Z"(f), components of the complex impedance for AVF as a function of the frequency (f) in a log-log plot. The figure shows that Z'(f) and Z"(f) remained overlapping at low frequency, while around 10 Hz, the curves separated and decreased continuously with the frequency. This behavior is typical of dielectric materials, representing that prevails the capacitive domain[25].

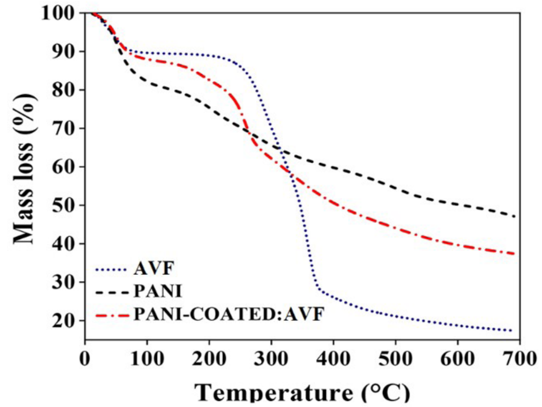

Figure 5. Thermogravimetric analysis (TGA) curves of samples AVF, PANI, and PANI-COATED:AVF.

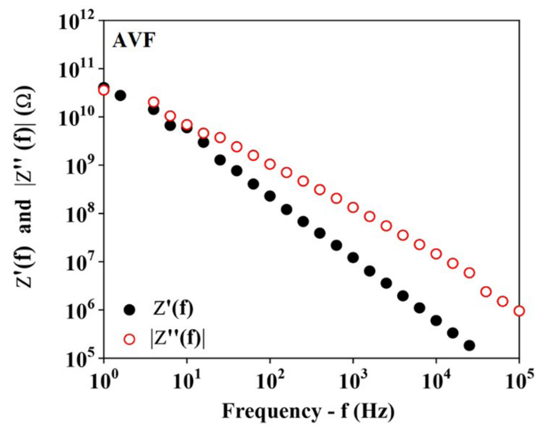

Figure 6. Real, Z'(f), and imaginary, Z''(f), components of the complex impedance versus frequency (f) of AVF.

Figure 7 shows Z'(f) and Z''(f) vs. f obtained from PANI (Figure 7a) and PANI-COATED:AVF, along with Argand diagrams for each (Figure 7b). The full-line curves of Figure 7 were derived from experimental-theoretical fittings using the Cole-Cole phenomenological model[26] which satisfied the principle of equivalence of a Maxwell circuit[27] represented by the empirical formula:

$$Z^{*}(\omega) = R/[1+(i\omega RC)^{\alpha}] \quad (1)$$

In this equation, ω is the angular frequency obtained by ω = 2πf, R is the dc electrical resistance, C is the electrical capacitance, and α is a parameter of dielectric relaxation that can assume values between 0 and 1; this shows that the distribution of relaxation times was highly symmetric[28,29].

Both impedance spectra in Figure 7 exhibit a plateau at about 40 kΩ (called the dc electrical resistance or R = Z'(f → 0)) which extends up to around 20 kHz; beyond this frequency, known as the critical frequency f_c[30], the Z''(f) shows a peak with a maximum height on the f_c. Therefore, the analogous behaviors of Z'(f) and Z''(f) between PANI (Figure 7a) and PANI-COATED:AVF (Figure 7b) imply that

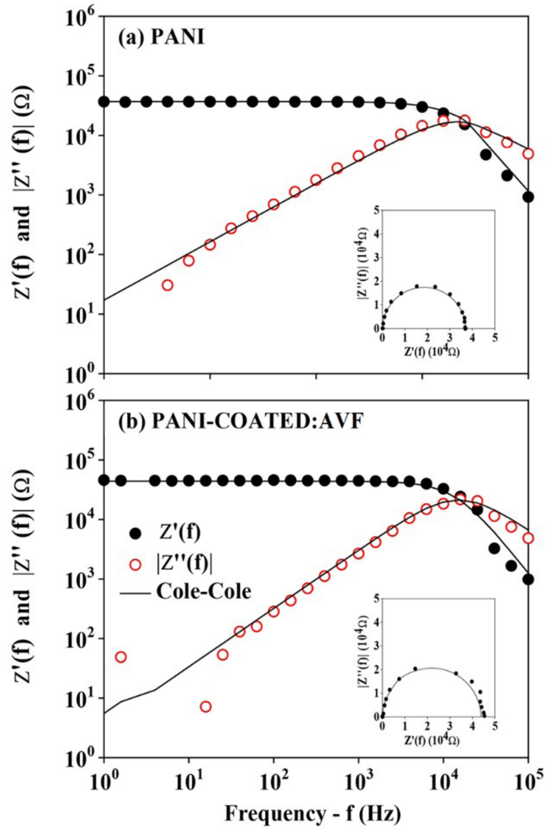

Figure 7. Z' and Z'' vs. f of (a) PANI and (b) PANI-COATED:AVF. The inset image shows an Argand diagram of the Z'(f) vs. Z''(f) of (a) PANI and (b) PANI-COATED:AVF. The full lines represent the experimental fittings obtained from Equation 1.

the PANI deposited on AVF acted as an efficient semiconductor coating[12,14]. The diagrams show the value of electrical resistance, through the diameter of the semicircles equal to 370 kΩ and 440 kΩ, respectively, to PANI (Figure 7a) and PANI-COATED:AVF (Figure 7b). Furthermore, the presence of a single semicircle indicates only one transport mechanism, as there is no interface effect[30].

The experimental-theoretical fitting using Equation 1 shows that α = (0.98 ± 0.01) and f_c = (20 ± 0.1) kHz remained practically constant, while R = (405 ± 35) kΩ and C = (0.26 ± 0.02) nF varied only slightly but remained in the same order of magnitude.

4. Conclusions

In this paper, SEM and AFM images showed that the surface smoothness of fibers increased after PANI synthesis; failures in the polymeric coating of PANI were shown by OM. However, the Z'(f) and Z''(f) indicated that these failures did not interfere with electrical conductivity, and demonstrated that the electrical properties attributed to AVF by PANI were not limited to the dc regime (f → 0). Furthermore, the use of the Cole-Cole model demonstrated that the samples presented a symmetric arc in a complex plane. The thermal results revealed that the AVF and the

PANI-COATED:AVF could be submitted to temperatures of up to around 200ºC and 300ºC, respectively, without severe degradation. Therefore, this research provides a stimulus for the investigation and fabrication of organic polymer-based devices capable of providing a high electrical performance while preserving the environment. Finally, compared to other VF, the efficient utilization of VFA can favor the fabrication of environmentally friendly polymer composites and generate employment and income for the riverside Amazon communities.

5. Author's Contribution

- **Conceptualization** – Rodrigo Fernando Bianchi; Cleidinéia Cavalcante da Costa.
- **Data curation** – Jefter Victor Gonçalves; Rodrigo Fernando Bianchi; Cleidinéia Cavalcante da Costa.
- **Formal analysis** – Jefter Victor Gonçalves; Rodrigo Fernando Bianchi; Cleidinéia Cavalcante da Costa.
- **Funding acquisition** – Rodrigo Fernando Bianchi.
- **Investigation** – Jefter Victor Gonçalves; Jefferson Suela; Marcus Vinícius Duarte Silva; Cleidinéia Cavalcante da Costa.
- **Methodology** – Jefter Victor Gonçalves; Jefferson Suela; Marcus Vinícius Duarte Silva; Cleidinéia Cavalcante da Costa.
- **Project administration** – Jefter Victor Gonçalves; Rodrigo Fernando Bianchi; Cleidinéia Cavalcante da Costa.
- **Resources** – Rodrigo Fernando Bianchi; Jefferson Suela; Marcus Vinícius Duarte Silva; Cleidinéia Cavalcante da Costa.
- **Software** – Jefter Victor Gonçalves; Rodrigo Fernando Bianchi; Cleidinéia Cavalcante da Costa.
- **Supervision** – Rodrigo Fernando Bianchi; Cleidinéia Cavalcante da Costa.
- **Validation** – Rodrigo Fernando Bianchi; Cleidinéia Cavalcante da Costa.
- **Visualization** – Jefter Victor Gonçalves; Rodrigo Fernando Bianchi; Cleidinéia Cavalcante da Costa.
- **Writing – original draft** – Jefter Victor Gonçalves; Jefferson Suela; Marcus Vinícius Duarte Silva; Rodrigo Fernando Bianchi; Cleidinéia Cavalcante da Costa.
- **Writing – review & editing** – Jefter Victor Gonçalves; Rodrigo Fernando Bianchi; Cleidinéia Cavalcante da Costa.

6. Acknowledgements

This work was supported by INEO, FAPEMIG (APQ-03165-17), CNPq (308185/2016-1) and CAPES (001).

7. References

1. Cavalcante, P. B. (1991). *Frutas comestíveis da Amazônia*. Belém: CNPq/Museu Paraense Emílio Goeldi.
2. Nogueira, O. L., Figueirêdo, F. J. C., & Müller, A. A. (Eds.). (2005). *Sistema de produção – açaí*. Belém: Embrapa Amazônia Oriental.
3. Muñiz-Miret, N., Vamos, R., Hiraoka, M., Montagnini, F., & Mendelsohn, R. O. (1996). The economic value of managing the acai palm (Euterpe oleracea mart.) in the floodplains of the Amazon estuary, Para, Brazil. *Forest Ecology and Management*, *87*(1-3), 163-173. http://dx.doi.org/10.1016/S0378-1127(96)03825-X.
4. Yamaguchi, K. K. L., Pereira, L. F. R., Lamarão, C. V., Lima, E. S., & Veiga-Junior, V. F. (2015). Amazon acai: chemistry and biological activities: a review. *Food Chemistry*, *179*, 137-151. http://dx.doi.org/10.1016/j.foodchem.2015.01.055. PMid:25722148.
5. Santos, N. S., Silva, M. R., & Alves, J. L. (2017). Reinforcement of a biopolymer matrix by lignocellulosic agro-waste. *Procedia Engineering*, *200*, 422-427. http://dx.doi.org/10.1016/j.proeng.2017.07.059.
6. Bufalino, L., Guimarães, A. A., Silva, B. M. S., Souza, R. L. F., Melo, I. C. N. A., Oliveira, D. N. P. S., & Trugilho, P. F. (2018). Local variability of yield and physical properties of açaí waste and improvement of its energetic attributes by separation of lignocellulosic fibers and seeds. *Journal of Renewable and Sustainable Energy*, *10*(5), 053102. http://dx.doi.org/10.1063/1.5027232.
7. Poletto, M., Ornaghi, H. L. Jr., & Zattera, A. J. (2014). Native cellulose: structure, characterization and thermal properties. *Materials*, *7*(9), 6105-6119. http://dx.doi.org/10.3390/ma7096105. PMid:28788179.
8. Razak, S. I. A., Rahman, W. A. W. A., Sharif, N. F. A., & Yahya, M. Y. (2012). Simultaneous numerical optimization of the mechanical and electrical properties of polyaniline coated kenaf fiber using response surface methodology: nanostructured polyaniline on natural fiber. *Composite Interfaces*, *19*(7), 411-424. http://dx.doi.org/10.1080/15685543.2012.757957.
9. Silva, C. K., Mastrantonio, D. J. S., Costa, J. A. V., & Morais, M. G. (2019). Innovative pH sensors developed from ultrafine fibers containing açaí (Euterpe oleracea). *Food Chemistry*, *294*, 397-404. http://dx.doi.org/10.1016/j.foodchem.2019.05.059. PMid:31126480.
10. Castro, C. D. P. C., Dias, C. G. B. T., & Faria, J. A. F. (2010). Production and evaluation of recycled polymers from açaí fibers. *Materials Research*, *13*(2), 159-163. http://dx.doi.org/10.1590/S1516-14392010000200007.
11. Tavares, F. F. C., Almeida, M. D. C., Silva, J. A. P., Araújo, L. L., Cardozo, N. S. M., & Santana, R. M. C. (2020). Thermal treatment of açaí (Euterpe oleracea) fiber for composite reinforcement. *Polímeros: Ciência e Tecnologia*, *30*(1), e2020003. http://dx.doi.org/10.1590/0104-1428.09819.
12. Araujo, J. R., Adamo, C. B., & De Paoli, M.-A. (2011). Conductive composites of polyamide-6 with polyaniline coated vegetal fiber. *Chemical Engineering Journal*, *174*(1), 425-431. http://dx.doi.org/10.1016/j.cej.2011.08.050.
13. Souza, F. G. Jr., Paiva, L. O., Michel, R. C., & Oliveira, G. E. (2011). Modificação da fibra de coco com polianilina e o seu uso como sensor de pressão. *Polímeros: Ciência e Tecnologia*, *21*(1), 39-46. http://dx.doi.org/10.1590/S0104-14282011005000016.
14. Souza, F. G. Jr., Picciani, P. H. S., Rocha, E. V., & Oliveira, G. E. (2010). Estudo das propriedades mecânicas e elétricas de fibras de curauá modificada com polianilina. *Polímeros: Ciência e Tecnologia*, *20*(5), 377-382. http://dx.doi.org/10.1590/S0104-14282010005000058.
15. Macdiarmid, A. G., Chiang, J. C., Richter, A. F., & Epstein, A. J. (1987). Polyaniline: a new concept in conducting polymers. *Synthetic Metals*, *18*(1-3), 285-290. http://dx.doi.org/10.1016/0379-6779(87)90893-9.

16. Costa, C. C., Mapa, L. M., Kelmer, A. C., Ferreira, S. O., & Bianchi, R. F. (2022). New insight into natural fiber-reinforced polymer composites as pressure sensors: experiment, theory, and application. *Polymer Composites*, *43*(12), 8869-8876. http://dx.doi.org/10.1002/pc.27068.
17. Costa, C. C. (2019). *Efeitos da pressão mecânica nas propriedades elétricas ac em compósitos elastoméricos a base de fibras naturais recobertas com polímero condutor* (Doctoral thesis). Universidade Federal de Viçosa, Viçosa.
18. Cantalice, J. D. A., Mazzini, E. G. Jr., Freitas, J. D., Silva, R. C., Faez, R., Costa, L. M. M., & Ribeiro, A. S. (2021). Polyaniline-based electrospun polycaprolactone nanofibers: preparation and characterization. *Polímeros: Ciência e Tecnologia*, *31*(1), e2021002. http://dx.doi.org/10.1590/0104-1428.09320.
19. Schauss, A. G., Wu, X., Prior, R. L., Ou, B., Patel, D., Huang, D., & Kababick, J. P. (2006). Phytochemical and nutrient composition of the freeze-dried Amazonian palm berry, *Euterpe oleraceae* Mart. (Acai). *Journal of Agricultural and Food Chemistry*, *54*(22), 8598-8603. http://dx.doi.org/10.1021/jf060976g. PMid:17061839.
20. Martins, M. A., Pessoa, J. D. C., Gonçalves, P. S., Souza, F. I., & Mattoso, L. H. C. (2008). Thermal and mechanical properties of the açaí fiber/natural rubber composites. *Journal of Materials Science*, *43*(19), 6531-6538. http://dx.doi.org/10.1007/s10853-008-2842-4.
21. Kumari, A., Singh, I., & Dixit, S. K. (2014). Effect of annealing on graphene incorporated poly-(3-hexylthiophene): $CuInS_2$ photovoltaic device. *AIP Conference Proceedings*, *1620*(1), 35-40. http://dx.doi.org/10.1063/1.4898216.
22. Epstein, A. J., Ginder, J. M., Zuo, F., Bigelow, R. W., Woo, H.-S., Tanner, D. B., Richter, A. F., Huang, W.-S., & MacDiarmid, A. G. (1987). Insulator-to-metal transition in polyaniline. *Synthetic Metals*, *18*(1-3), 303-309. http://dx.doi.org/10.1016/0379-6779(87)90896-4.
23. Zhou, W., Zhu, D., Langdon, A., Li, L., Liao, S., & Tan, L. (2009). The structure characterization of cellulose xanthogenate derived from the straw of Eichhornia crassipes. *Bioresource Technology*, *100*(21), 5366-5369. http://dx.doi.org/10.1016/j.biortech.2009.05.066. PMid:19540749.
24. Mostafaei, A., & Zolriasatein, A. (2012). Synthesis and characterization of conducting polyaniline nanocomposites containing ZnO nanorods. *Progress in Natural Science: Materials International*, *22*(4), 273-280. http://dx.doi.org/10.1016/j.pnsc.2012.07.002.
25. Santos, M. C., Bianchi, A. G. C., Ushizima, D. M., Pavinatto, F. J., & Bianchi, R. F. (2017). Ammonia gas sensor based on the frequency-dependent impedance characteristics of ultrathin polyaniline films. *Sensors and Actuators A: Physical*, *253*, 156-164. http://dx.doi.org/10.1016/j.sna.2016.08.005.
26. Cole, K. S., & Cole, R. H. (1941). Dispersion and absorption in dielectrics I. Alternating current characteristics. *The Journal of Chemical Physics*, *9*(4), 341-351. http://dx.doi.org/10.1063/1.1750906.
27. Macdonald, J. R. (1999). Dispersed electrical-relaxation response: discrimination between conductive and dielectric relaxation processes. *Brazilian Journal of Physics*, *29*(2), 332-346. http://dx.doi.org/10.1590/S0103-97331999000200014.
28. Macdonald, J. R. (1992). Impedance spectroscopy. *Annals of Biomedical Engineering*, *20*(3), 289-305. http://dx.doi.org/10.1007/BF02368532. PMid:1443825.
29. Barsoukov, E., & Macdonald, J. R. (Eds.). (2005). *Impedance spectroscopy theory, experiment, and applications*. Hoboken: John Wiley & Sons, Inc. http://dx.doi.org/10.1002/0471716243.
30. Gonçalves, G., Pimentel, A., Fortunato, E., Martins, R., Queiroz, E. L., Bianchi, R. F., & Faria, R. M. (2006). UV and ozone influence on the conductivity of ZnO thin films. *Journal of Non-Crystalline Solids*, *352*(9-20), 1444-1447. http://dx.doi.org/10.1016/j.jnoncrysol.2006.02.021.

Received: Jul. 18, 2022
Revised: Jul. 01, 2023
Accepted: Jul. 11, 2023